

# Mathematical Modelling and Correlation Between the Primary Waviness and Roughness Profiles During Hard Turning

Mite Tomov<sup>a\*</sup>, Bojan Prangoski<sup>a</sup>, Pawel Karolczak<sup>b</sup>

<sup>a</sup>Faculty of Mechanical Engineering-Skopje, Ss Cyril and Methodius" University in Skopje, Karpos II, 1000 Skopje, North Macedonia.

<sup>b</sup>Department of Machine Tools and Mechanical Technologies, Wroclaw University of Science and Technology, 50-370 Wroclaw, Poland

Received April 13 2021

Accepted June 23 2021

## Abstract

This paper presents a research primarily aimed at determining the correlations between the primary profile, waviness, and roughness profiles during hard turning, using mathematical modeling of the primary profile (Pa), the roughness profile (Ra) and the waviness profile (Wa). For this purpose, we employed the Design of experiments (DOE) principles expressing the roughness parameters models as a nonlinear function shape of the first order of the input variables: cutting speed ( $v$ ), feed ( $f$ ), depth of cut ( $a_p$ ) and tool nose radius ( $r_e$ ). The models were done based on empirical data obtained by processing special rings made of steel IEN C55 (AISI 1055) with hardness of  $53 \pm 1$  HRC, using a CNC lathe. The obtained results are presented as mathematical models, but also as 3D diagrams which clearly show the change trends and their mutual relationships for the considered parameters.

© 2021 Jordan Journal of Mechanical and Industrial Engineering. All rights reserved

**Keywords:** hard turning, surface roughness, primary profile, waviness profile, roughness profiles, mathematical modeling;

## 1. Introduction

C.L. He and all. in the research presented in [1] provide a detailed overview of the State-of-the-art of the influential factors and the applied methods used in surface roughness modeling in turning, regardless of whether the processed materials have normal or enhanced hardness. It is worth noting that when processing materials with enhanced hardness, i.e., hardness greater than 45 HRC, more and more attempts are made to replace grinding with turning [2-4]. Therefore, there is much research referring to hard turning surface roughness modelling and predicting. Agrawal A. and all., in [5] provide a table overview of the literature review of optimization studies on hard turning. Thus, [5-8] provide results of the impact of cutting parameters (cutting speed, feed and depth of cut) when optimizing and predicting the roughness of the surfaces, using the regression analysis technique, while the research [9-10] also analyze the impact of cutting speed, feed and depth of cut, but using the *Taguchi experimental design*. Research referring to, among other things, how tool geometry impacts the predicting of surface roughness during hard turning can also be found in [11,12]. The influence of the cutting tool materials on the roughness optimization is analyzed in [13-15], while the influence of the workpiece hardness on the roughness profile formation during hard turning is analyzed in [4,16-18]. Information on the impact of different cooling mediums is provided in the research in [19, 20].

A detailed analysis of the aforementioned research suggests that, regardless of the input parameters in the research (cutting parameters, tool geometry, cutting tool materials, workpiece hardness etc.), surface roughness optimization and prediction during hard turning is done for very few parameters, typically the Ra and Rz (Rt) parameters. This trend of replacing the term surface roughness with the Ra parameter continues even today when researching the processing of new materials [21,22] or when controlling complex machine parts [23].

Knowing that the roughness profile derives from the primary profile and total profile by applying appropriate filtering techniques [24], it is worth noting that the research [2-20] lacks information on waviness deviation and form deviation of the pieces, crucial values for the proper functioning of the parts.

This research aims at determining whether any correlation exists between the primary profile (P-profile), the waviness profile (W-profile), and the roughness profile (R-profile) during hard turning. This is very important because the primary profile, the waviness profile, and the roughness profile coexist and together they form the surface profile (the total profile) as a 2D representation of the surface topography. The justification of this research arises also from the fact that, according to DIN 4760, from a structural point of view, we can simultaneously define six types of deviations including waviness (2<sup>nd</sup> order deviation) and roughness (3<sup>rd</sup> to 5<sup>th</sup> order deviation). We will analyze the correlation between the primary profile, the waviness profile, and the roughness profile using mathematical models for modelling the Pa, Wa, and Ra parameters.

\* Corresponding author e-mail: mite.tomov@mf.edu.mk.



the work rings to obtain the statistically significant data for the test. A pick-up stylus used had a top angle of  $60^\circ$  and a top radius of  $2\text{ }\mu\text{m}$ . A skidless pick-up was used. During the measurements, the instrument was mechanically leveled

with respect to the measured surface. The measuring system was calibrated using a type C etalon with  $R_a=2.97\text{ }\mu\text{m}$ , and was verified using a type C etalon with  $R_a=6\text{ }\mu\text{m}$ . The used calibration etalons have a measuring uncertainty of 5%.

**Table 1:** Measurement conditions of primary, waviness and roughness profiles.

Profile/Parameters	Primary profile / $P_a$ / SE	
Experiment No.	All	
Filter	Gaussian	
$r_{up}(\mu\text{m})$	2	
$\lambda_s$ profile filter ( $\mu\text{m}$ )	2.5	
L evaluation length	8	
$L = 1 \times N$ (mm)		
Profile/Parameters	Waviness profile / $W_a$	
Experiment No.	1,2,5,6,9,10,13,14	3,4,7,8,11,12,15,16,17,18,19,20
Filter	Gaussian	
$r_{up}(\mu\text{m})$	2	
$\lambda_c$ profile filter (mm)	0.25	0.8
$\lambda_f$ profile filter (mm)	2.5	
L evaluation length (mm)	$5 \times 2.5 = 12.5$	
Profile/Parameters	Roughness profile / $R_a$	
Experiment No.	1,2,5,6,9,10,13,14	3,4,7,8,11,12,15,16,17,18,19,20
Filter	Gaussian	
$r_{up}(\mu\text{m})$	2	
$\lambda_s$ profile filter ( $\mu\text{m}$ )	2.5	
$\lambda_c$ profile filter (mm)	0.25	0.8
$l_r$ sampling length		
$l_n$ evaluation length	$5 \times 0.25 = 1.25$	$5 \times 0.8 = 4$
$l_n = N \times l_r$ (mm)		

**Table 2.** Experimental plan and results.

No.	$V$ (m/min)	$f$ (mm/rev)	$a_p$ (mm)	$r_e$ (mm)	$P_a$ ( $\mu\text{m}$ )	$W_a$ ( $\mu\text{m}$ )	$R_a$ ( $\mu\text{m}$ )	SE <i>P-profile</i>
1	100	0.09	0.2	0.4	0.726	0.055	0.695	0.036
2	200	0.09	0.2	0.4	0.772	0.049	0.735	0.047
3	100	0.2	0.2	0.4	3.447	0.078	3.398	0.033
4	200	0.2	0.2	0.4	3.407	0.094	3.362	0.044
5	100	0.09	0.4	0.4	0.749	0.076	0.720	0.033
6	200	0.09	0.4	0.4	0.821	0.055	0.782	0.041
7	100	0.2	0.4	0.4	3.347	0.080	3.309	0.038
8	200	0.2	0.4	0.4	3.501	0.101	3.442	0.051
9	100	0.09	0.2	1.2	0.258	0.045	0.249	0.147
10	200	0.09	0.2	1.2	0.317	0.054	0.287	0.078
11	100	0.2	0.2	1.2	0.944	0.036	0.938	0.047
12	200	0.2	0.2	1.2	0.949	0.040	0.934	0.047
13	100	0.09	0.4	1.2	0.284	0.042	0.254	0.115
14	200	0.09	0.4	1.2	0.236	0.041	0.218	0.141
15	100	0.2	0.4	1.2	0.958	0.035	0.938	0.039
16	200	0.2	0.4	1.2	0.956	0.036	0.940	0.054
17	141.4	0.134	0.283	0.8	0.700	0.026	0.699	0.039
18	141.4	0.134	0.283	0.8	0.732	0.027	0.726	0.043
19	141.4	0.134	0.283	0.8	0.726	0.028	0.713	0.032
20	141.4	0.134	0.283	0.8	0.788	0.036	0.781	0.042

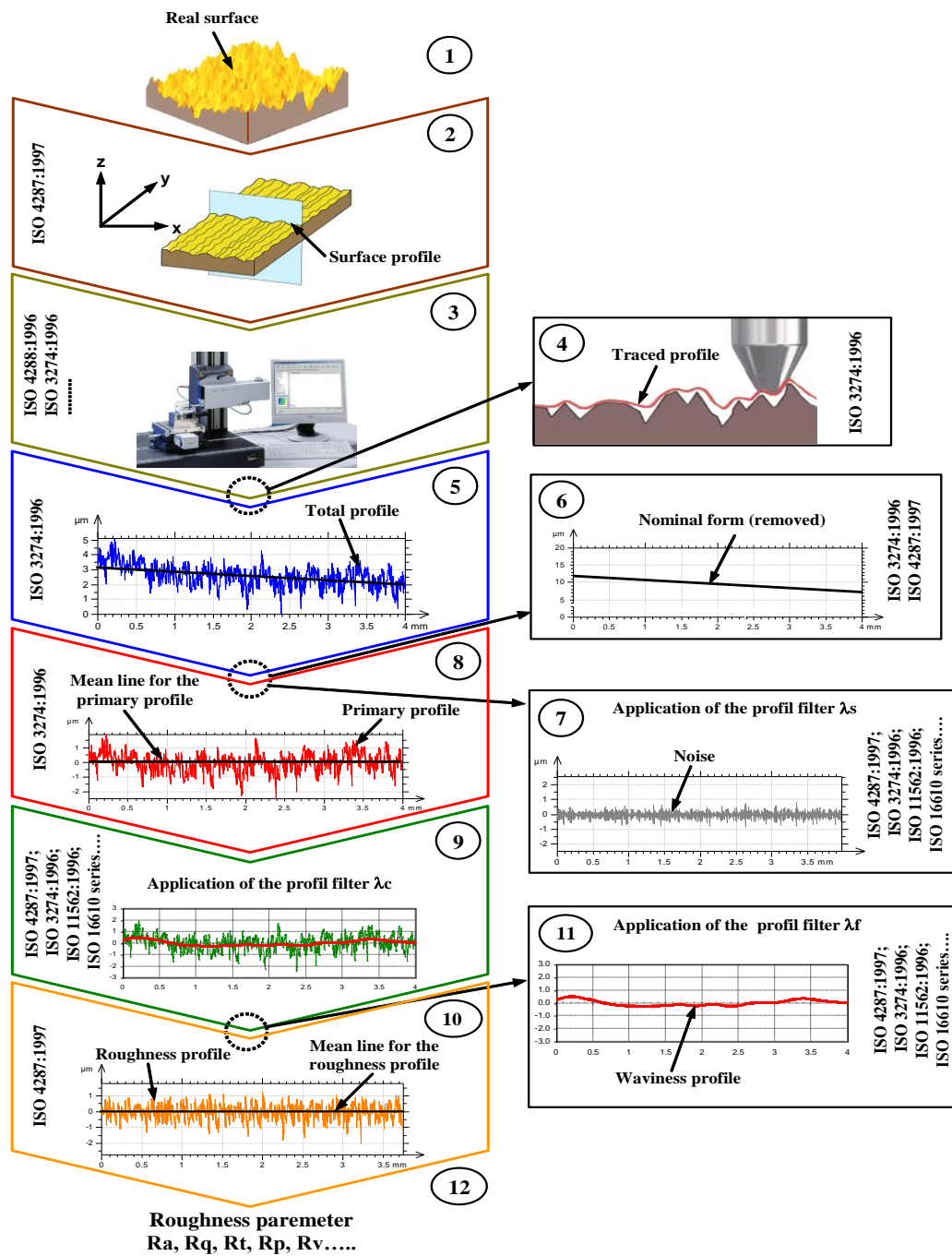


Figure 3. Procedure for obtaining the primary profile, the roughness profile, and the waviness profile [24]

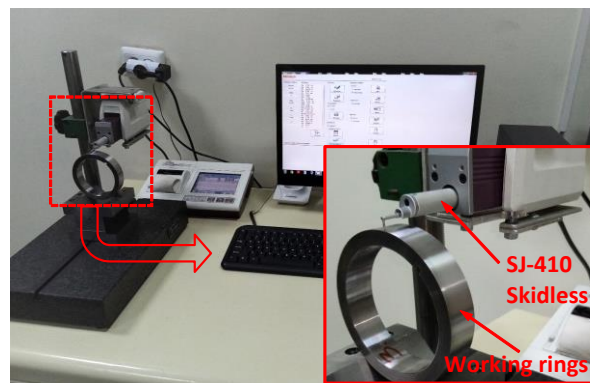


Figure 4. Surf test model No. SJ-410 (Mitutoyo make).

#### 4. Results and discussion

The entire plan for the realization of the experiments, as well as the measured values for the parameters  $P_a$ ,  $W_a$ ,  $R_a$  and  $SE$  is presented in Table 2. The value of all parameters provided in Table 2 are mean values of five measurements.

The following mathematical models for the considered parameters were obtained based on the value from Table 2 and applying the methodology stipulated in point 2:

$$P_a = 15.259 \cdot v^{0.0379652} \cdot f^{1.722} \cdot a^{-0.0155956} \cdot r_\varepsilon^{-1.054} \quad (2)$$

$$W_a = 0.0406614 \cdot v^{0.0491459} \cdot f^{0.1290388} \cdot a^{0.0104809} \cdot r_\varepsilon^{-0.5093038} \quad (3)$$

$$R_a = 17.175 \cdot v^{0.0278376} \cdot f^{1.783} \cdot a^{-0.0278446} \cdot r_\varepsilon^{-1.071} \quad (4)$$

$$SE = 0.0095850 \cdot v^{0.1733292} \cdot f^{-0.5450216} \cdot a^{0.0656300} \cdot r_\varepsilon^{0.5575011} \quad (5)$$

The mathematical models expressed by the equations (2-5) represent first order models without mutual interaction

and without factor significance evaluation. Their dispersion analysis together with an adequacy evaluation is provided in Table 3.

For the  $W_a$  parameter, the data in Table 3 suggest that the coefficient of determination is 0.64 which justifies its use in the first order model with mutual interaction. We decided to use a model without mutual interaction in order to enable the comparability with the models of the other considered parameters and because of the affirmative assessment of the adequacy.

The minus sign in the exponent in the term of the model indicates an inverse relationship between that term of the model and the modeled parameter.

In order to provide a graphic overview of the obtained mathematical models of the modeled parameters of the investigated hyperspace, the paper presents 3D graphs, Figures 5-8.

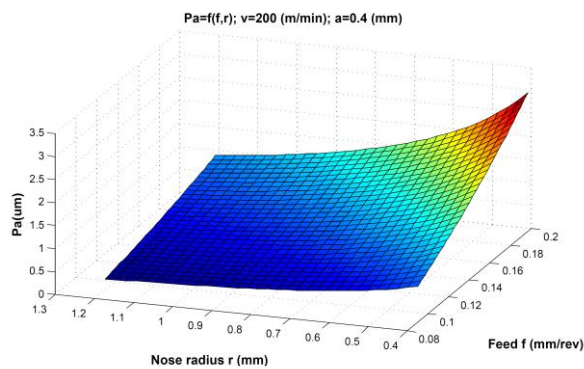


Figure 5. 3D graph for  $P_a$ , according to equation (2)

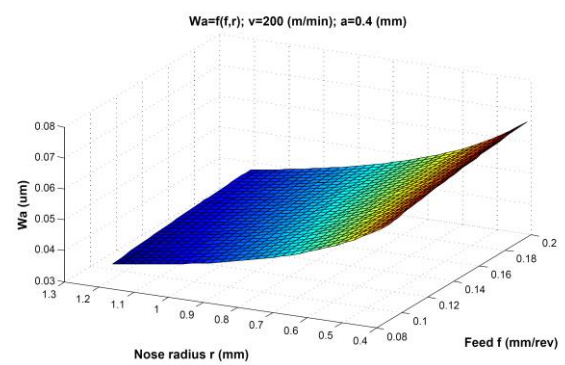


Figure 6. 3D graph for  $W_a$ , according to equation (3)

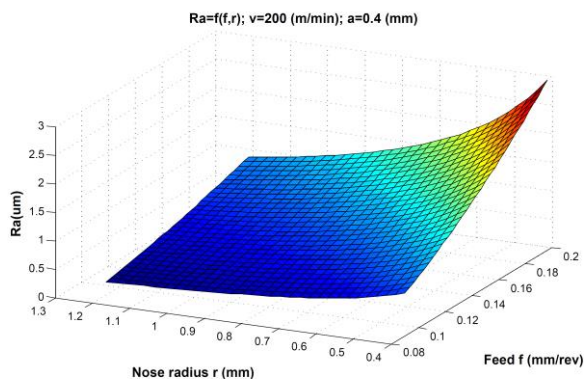


Figure 7. 3D graph for  $R_a$ , according to equation (4)

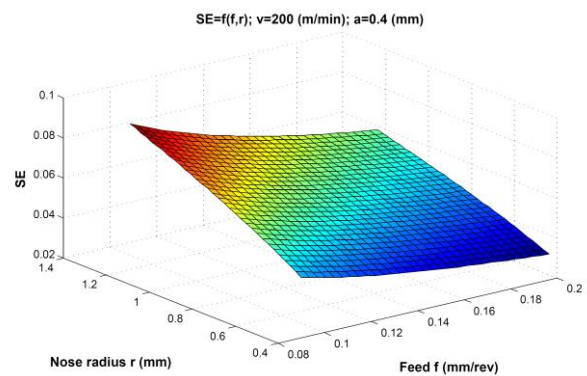


Figure 8. 3D graph for  $SE$ , according to equation (5)



If we compare the mathematical models for the  $Pa$  and the  $Ra$  parameters, equations (2) and (4), we will note a great similarity with respect to the input variables constants and exponents. There the feed ( $f$ ) and the tool nose radius ( $r_e$ ) have a dominant influence. The increase of the cutting speed and the reduction of the depth of cut, although not significant, can contribute to the increase of the values of  $Pa$  and  $Ra$ . Figure 9 presents a 3D diagram showing the modelled surfaces for the  $Pa$  and  $Ra$  parameters. Figure 9 clearly demonstrates that  $Pa$  and  $Ra$  behave identically throughout the investigated hyperspace.

If we analyze the mathematical model for the Wa parameter, we will also conclude that the feed ( $f$ ) and the tool nose radius ( $r_{\varepsilon}$ ) have a dominant influence. However, their influence, especially the influence of  $f$  is significantly reduced, as shown by the value of their exponents. The comparison between the Ra mathematical model and the Wa mathematical model shows and increased influence of the cutting speed ( $v$ ) and a sign change of the exponent for

the depth of cut ( $a_p$ ). Although, according to DIN 4760, the causes of 2<sup>nd</sup> order deviations (waviness) do not include the feed ( $f$ ), the tool nose radius ( $r_\epsilon$ ), the cutting speed ( $v$ ) and the depth of cut ( $a_p$ ), when combined they can still cause some tool vibrations or elastic deformations on the work piece, which can directly impact the waviness.

It is interesting to compare the Wa mathematical model and the SE mathematical model, equations (3) and (5), Figure 10. The increase of the value of  $f$  can increase the value of Wa and reduce the value of SE, i.e., the increase of the  $r_e$  value leads to a reduction of the Wa and an increase of the SE. This suggests that while waviness decreases, the stochastic character of the primary profile and the roughness profile, expressed by the SE parameter, increases. Still, we need to mention that the waviness profile derives from the mean line of the primary profile. The mean line of primary profile is obtained using profile filters. Any “imperfection” in obtaining the mean line does influence the shape of the waviness profile.

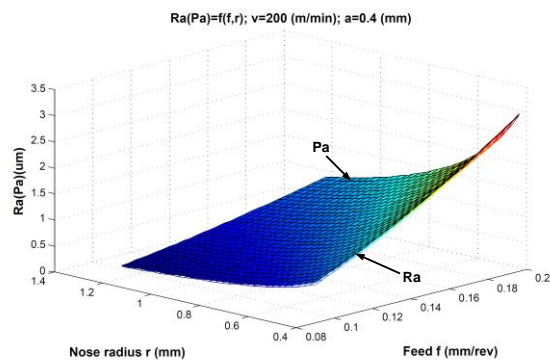


**Figure 9.** 3D graph for correlation between Pa and Ra

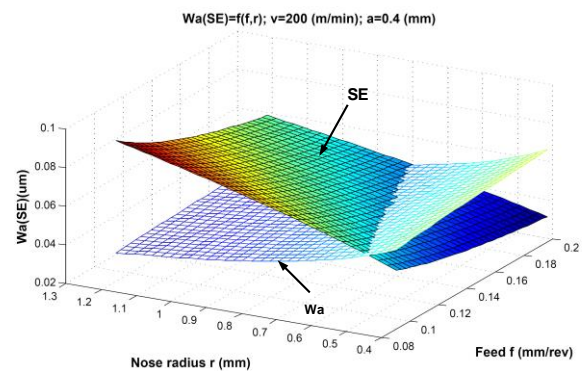


**Figure 10.** 3D graph for correlation between Wa and SE

**Table 3.** Dispersion analysis

		Degrees of freedom f	Sum of squares s	Dispersion s/f	Dispersion ratios fr	Table value ft	Model adequacy evaluation
Pa	Residual sum	15	0.264080	0.017605			
	Experiment error	3	0.007536	0.002512			
	Model adequacy	12	0.256544	0.021379	8.510	8.740	fr<ft adequate
	Multiple regression coefficient: R=0.9899						
Ra	Residual sum	15	0.198609	0.013241			
	Experiment error	3	0.007023	0.002341			
	Model adequacy	12	0.191586	0.015966	6.820	8.740	fr<ft adequate
	Multiple regression coefficient: R=0.9928						
Wa	Residual sum	15	1.889	0.125933			
	Experiment error	3	0.065015	0.021672			
	Model adequacy	12	1.824	0.151998	7.014	8.740	fr<ft adequate
	Multiple regression coefficient: R=0.6384						
SE	Residual sum	15	1.779	0.118613			
	Experiment error	3	0.053990	0.017997			
	Model adequacy	12	1.725	0.143767	7.988	8.740	fr<ft adequate
	Multiple regression coefficient: R=0.7526						

## 5. Conclusion

The research presented in this paper showed that there is a strict correlation between the primary profile (P-profile), the waviness profile (W-profile) and the roughness profile (R-profile) during hard turning. The SE parameter, particularly its small values, shows the stability of the hard turning process employed in this research. The great similarity between the Pa and the Ra parameters, especially the small value for the Wa parameter for all 20 experiments, perhaps provides the justification for emphasizing the roughness profile and the roughness parameters when modeling the geometric structure of the surface.

## Acknowledgments

The authors of this paper would like to use this opportunity to express a great deed of gratitude to prof. Mikolaj Kuzinovski Ph.D (in memoriam) for the invaluable contribution to the realization of the research in this study, "ZM RezniAlati DOO -Skopje" (representative in Republic North Macedonia for the Tungaloy Corporation company) for the donated turning tools used in the research, as well as to the company "SVEMEK DOOEL-Skopje" for the technical assistance provided in the processing of the work pieces and measuring the surface roughness.

## References

- [1]. C.L. He, W.J. Zong, J.J. Zhang, "Influencing factors and theoretical modeling methods of surface roughness in turning process: State-of-the-art". *International Journal of Machine Tools and Manufacture* 129 (2018) 15–26.
- [2]. Bartaryaa G., Choudhuryb S.K., "Effect of cutting parameters on cutting force and surface roughness during finish hard turning AISI52100 grade steel". *Procedia CIRP* 1, 2012, 651–656.
- [3]. Mohruni A.S., Yanis M., Edwin K., "Development of surface roughness prediction model for hard turning on AISI D2 steel using cubic boron nitride insert". *Jurnal Teknologi (Sciences & Engineering)*, 2018, 80(1), 173–178.
- [4]. Kumar S, Singh D, Kalsi NS., "Surface quality evaluation of AISI 4340 steel having varying hardness during machining with TiN-coated CBN inserts". *Journal of Engineering Tribology* 2016; 231 (7):925–933.
- [5]. Agrawal A, Goel S, Rashid W Bin, Price M. "Prediction of surface roughness during hard turning of AISI 4340 steel (69 HRC)". *Applied Soft Computing Journal* 2015; 30: 279–286.
- [6]. Bartaryaa G., Choudhuryb S.K., "Effect of cutting parameters on cutting force and surface roughness during finish hard turning AISI52100 grade steel". *Procedia CIRP* 1, 2012, 651–656.
- [7]. Panda, A., Sahoo, A.K., Rout, A.K., "Investigations on surface quality characteristics with multi-response parametric optimization and correlations". *Alexandria Engineering Journal*, 2016, 55, 1625–1633.
- [8]. Xio Z, Lio X, Long Z, Li M., "Effect of cutting parameters on surface roughness using orthogonal array in hard turning of AISI 1045 steel with YT5 tool". *International Journal of Advanced Manufacturing Technology* 2017; 93:273–282.
- [9]. Das SR, Panda A, Dhupal D., "Experimental investigation of surface roughness, flank wear, chip morphology and cost estimation during machining of hardened AISI 4340 steel with coated carbide insert". *Mechanics of Advanced Materials and Modern Processes* 2017; 3:1–14.
- [10]. J. Jena, A. Panda, A. K. Behera, P. C. Jena, Sudhansu Ranjan Das, D. Dhupal, "Modeling and Optimization of Surface Roughness in Hard Turning of AISI 4340 Steel with Coated Ceramic Tool". *Innovation in Materials Science and Engineering, Proceedings of ICEMIT 2017*, 2. 151–160.
- [11]. Meddour I, Yallese MA, Khattabi R, Elbah M, Boulanour L., "Investigating and modeling of cutting forces and surface roughness when hard turning of AISI 52100 steel with mixed ceramic tool: cutting conditions optimization". *International Journal of Advanced Manufacturing Technology* 2015;77:1387–1399.
- [12]. Zerti O, Yallese MA, Khattabi R, Chaoui K, Mabrouki T. "Design optimization for minimum technological parameters when dry turning of AISI D3 steel using Taguchi method". *International Journal of Advanced Manufacturing Technology* 2016; 89:1915–1934.
- [13]. Khellaf A, Aouici H, Smaiah S, Boutabba S, Yallese MA, Elbah M., "Comparative assessment of two ceramic cutting tools on surface roughness in hard turning of AISI H11 steel: including 2D and 3D surface topography". *International Journal of Advanced Manufacturing Technology* 2016; 89:333–354.
- [14]. Kacal A, Yildirim F., "Application of grey relational analysis in high-speed machining of hardened AISI D6 steel". *Journal of Mechanical Engineering Science* 2012; 227:1566–1576.
- [15]. Gunay M, Yucel E., "Application of Taguchi method for determining optimum surface roughness in turning of high-alloy white cast iron". *Measurement* 2013; 46:913–919.
- [16]. Tang L, Gao C, Huang J, Shen H, Lin X., "Experimental investigation of surface integrity in finish dry hard turning of hardened tool steel at different hardness levels". *International Journal of Advanced Manufacturing Technology* 2015; 77:1655–1669.
- [17]. Derakhshan E.D., Akbari A.A., "Experimental investigation on the effect of workpiece hardness and cutting speed on surface roughness in hard turning with CBN tools". *Proceedings of the World Congress on Engineering 2009 Vol II WCE 2009, July 1 - 3, 2009, London, U.K.*
- [18]. Mia M, Dhar NR., "Optimization of surface roughness and cutting temperature in high-pressure coolant-assisted hard turning using Taguchi method". *International Journal of Advanced Manufacturing Technology* 2017; 88:739–753.
- [19]. Chinchankar S, Salve AV, Netake P, More A, Kendre S, Kumar R., "Comparative evaluations of surface roughness during hard turning under dry and with water-based and vegetable oil-based cutting fluids". *Procedia Materials Science* 2014; 5:1966–1975.
- [20]. Naigade DM, Patil DK, Sadaiah M., "Some investigations in hard turning of AISI 4340 alloy steel in different cutting environments by CBN insert". *International Journal of Machining and Machinability of Materials* 2013; 14:165–193.
- [21]. Khannaa N., Agrawal C., Dograb M., Pruncuc C.I., "Evaluation of tool wear, energy consumption, and surface roughness during turning of inconel 718 using sustainable machining technique". *Journal of Materials Research and Technology* 2020; 9(3); 5794–5804.
- [22]. Kannan A, Mohan R, Viswanathan R, Sivashankar N. Experimental investigation on surface roughness, tool wear and cutting force in turning of hybrid (Al7075+SiC+Gr) metal matrix composites. *Journal of Materials Research and Technology* 2020; 9(6); 16529–16540.
- [23]. Tian F.C., Jiang H., Chen C., Accurate Modeling and Numerical Control Machining for Spiral Rotor of Double Rotor. *Jordan Journal of Mechanical and Industrial Engineering (JJMIE)* 2021; 15 (1); 15–21.
- [24]. TomovM, KuzinovskiM, CichoszP, "A new parameter of statistic equality of sampling lengths in surface roughness measurement". *Strojnicki Vestnik* 2013; 59(5):339–348.